

# The identification of myriocin-binding proteins

James K Chen<sup>1\*</sup>, William S Lane<sup>2</sup> and Stuart L Schreiber<sup>1</sup>

**Background:** Myriocin is a natural product that potently induces apoptosis of a murine cytotoxic T lymphocyte cell line (CTLL-2) and inhibits a serine palmitoyltransferase (SPT) activity that has been detected in cell extracts and is thought to initiate sphingolipid biosynthesis. Because SPT has never been biochemically purified and a comprehensive appraisal of myriocin-binding proteins has not been conducted, we isolated specific targets using myriocin-based affinity chromatography.

**Results:** Myriocin derivatives were synthesized and evaluated using CTLL-2 proliferation and SPT activity assays. Guided by these results, affinity chromatography matrices were prepared and two specific myriocin-binding proteins were isolated from CTLL-2 lysates. Analyses of these polypeptides establish conclusively that they are murine LCB1 and LCB2, mammalian homologs of two yeast proteins that have been genetically linked to sphingolipid biosynthesis.

**Conclusions:** The ability of myriocin-containing matrices to bind factors that have SPT activity and the exclusive isolation of LCB1 and LCB2 as myriocin-binding proteins demonstrates that the two proteins are directly responsible for SPT activity and that myriocin acts directly upon these polypeptides.

Addresses: <sup>1</sup>Howard Hughes Medical Institute, Department of Chemistry and Chemical Biology, Harvard University, 12 Oxford Street, Cambridge, MA 02138, USA. <sup>2</sup>Harvard Microchemistry Facility, Harvard University, 16 Divinity Avenue, Cambridge, MA 02138, USA.

\*Present address: Howard Hughes Medical Institute, Department of Molecular Biology and Genetics, John Hopkins University of Medicine, PCTB 701, 725 North Wolfe Street, Baltimore, MD 21205, USA.

Correspondence: Stuart L Schreiber  
E-mail: sls@slsiris.harvard.edu

**Key words:** affinity chromatography, LCB1, LCB2, myriocin, serine palmitoyltransferase

Received: 30 December 1998  
Revisions requested: 27 January 1999  
Revisions received: 1 February 1999  
Accepted: 2 February 1999

Published: 19 March 1999

Chemistry & Biology April 1999, 6:221–235  
<http://biomednet.com/elecref/1074552100600235>

© Elsevier Science Ltd ISSN 1074-5521

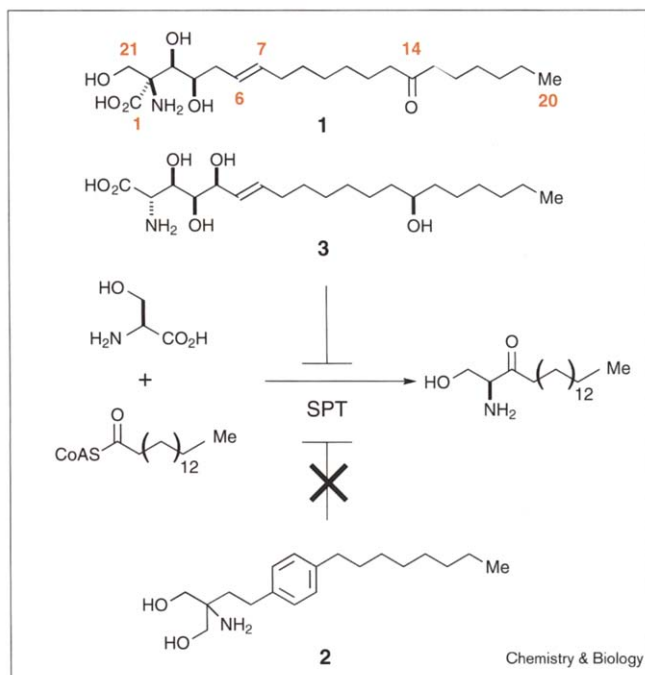
## Introduction

Myriocin (1; Figure 1), also known as thermozymocidin and ISP-1, is a sphingosine-like natural product, initially characterized as an antifungal metabolite of the thermophilic molds *Mycelia sterilia* and *Myriococcum albomyces* [1,2]. Screening programs for immunosuppressants have recently re-isolated myriocin from *Isaria sinclairii*, a fungus traditionally used in Chinese medicine for eternal youth [3]. The natural product potently inhibits lymphocyte proliferation in mouse allogeneic mixed lymphocyte reactions (MLRs), T cell-dependent antibody production, and the generation of alloreactive cytotoxic T lymphocytes. In these *in vitro* and *in vivo* assays, myriocin is equipotent to FK506 and approximately 10- to 100-fold more potent than cyclosporin A, two clinically prescribed immunosuppressants. The possible therapeutic efficacy of myriocin has sparked a renewed interest in this natural product, prompting a resurgence in synthetic and biological investigations of myriocin and its analogs. Furthermore, re-analysis of *M. sterilia* fermentation broths has yielded additional immunosuppressive metabolites called mycostericins, which are structurally related to myriocin [4–6].

Elucidating the biological mechanism of myriocin has therefore been an area of active research. Initial studies have demonstrated that myriocin is mechanistically distinct from FK506 and cyclosporin A. It does not block interleukin 2

(IL-2) production by antigen- or mitogen-stimulated T cells, but potently inhibits the proliferation of CTLL-2 cells, a murine cytotoxic T lymphocyte line that is IL-2 dependent [3]. Although this observation initially prompted speculation that myriocin might specifically abrogate IL-2 receptor-mediated signaling, subsequent studies by Nakamura *et al.* [7] and our laboratory (data not shown) indicate otherwise. Many transformed cell lines, including several other IL-2 dependent cell types, are not affected by myriocin, suggesting that myriocin is merely specific for certain lymphocyte lineages. Structural similarities between myriocin and sphingosine-derived molecules also suggest that myriocin might perturb sphingolipid biosynthetic or signaling pathways, and experimental support for this hypothesis has been obtained by two independent laboratories. Riezman and coworkers [8] reported that myriocin abrogates ceramide synthesis in *Saccharomyces cerevisiae* and ultimately causes cell death. A more precise mechanism for this general effect on ceramide production was then determined by Miyake *et al.* [9], who established that myriocin inhibits a serine palmitoyltransferase (SPT) activity that can be detected in CTLL-2-derived microsomes with an inhibition constant of 280 pM.

SPT is a membrane-associated activity that catalyzes the formation of 3-ketodihydrosphingosine from serine and palmitoyl CoA in a pyridoxal 5'-phosphate (PLP)-dependent

**Figure 1**

Effects of myriocin (1), FTY720 (2) and sphingofungin B (3) on serine palmitoyltransferase (SPT) activity. The numbering system for the carbon skeleton of myriocin is shown.

manner (Figure 1) [10–14]. Because SPT is the rate-limiting step in sphingolipid biosynthesis (Figure 2) and sphingolipid metabolites are important mediators of cellular proliferation and programmed cell death, it is conceivable that myriocin-induced perturbations might degrade the cellular immune response. In agreement with this hypothesis, micromolar concentrations of dihydrosphingosine, sphingosine or sphingosine 1-phosphate — downstream metabolites in the biosynthetic pathway — are able to suppress the effects of myriocin on CTLL-2 cells [9]. Sphingomyelinase and C2-ceramide also effect partial restoration of cell proliferation. Of these compounds, sphingosine 1-phosphate rescues the cells most effectively, and more recent studies have extended these findings, revealing that myriocin actually induces CTLL-2 programmed cell death and that high levels of exogenous sphingosine can also cause apoptosis [7]. Despite these provocative observations, a direct connection between SPT inhibition and immunosuppression remains to be demonstrated. The ability of sphingosine and sphingosine 1-phosphate to protect CTLL-2 cells from myriocin-induced apoptosis does not necessarily indicate that intracellular sphingolipid depletion is the cause of programmed cell death. Previous studies clearly show that sphingosine 1-phosphate can generally suppress apoptosis induced by a variety of stressors, and sphingosine is known to be phosphorylated rapidly upon introduction to cells [15–17]. Furthermore,

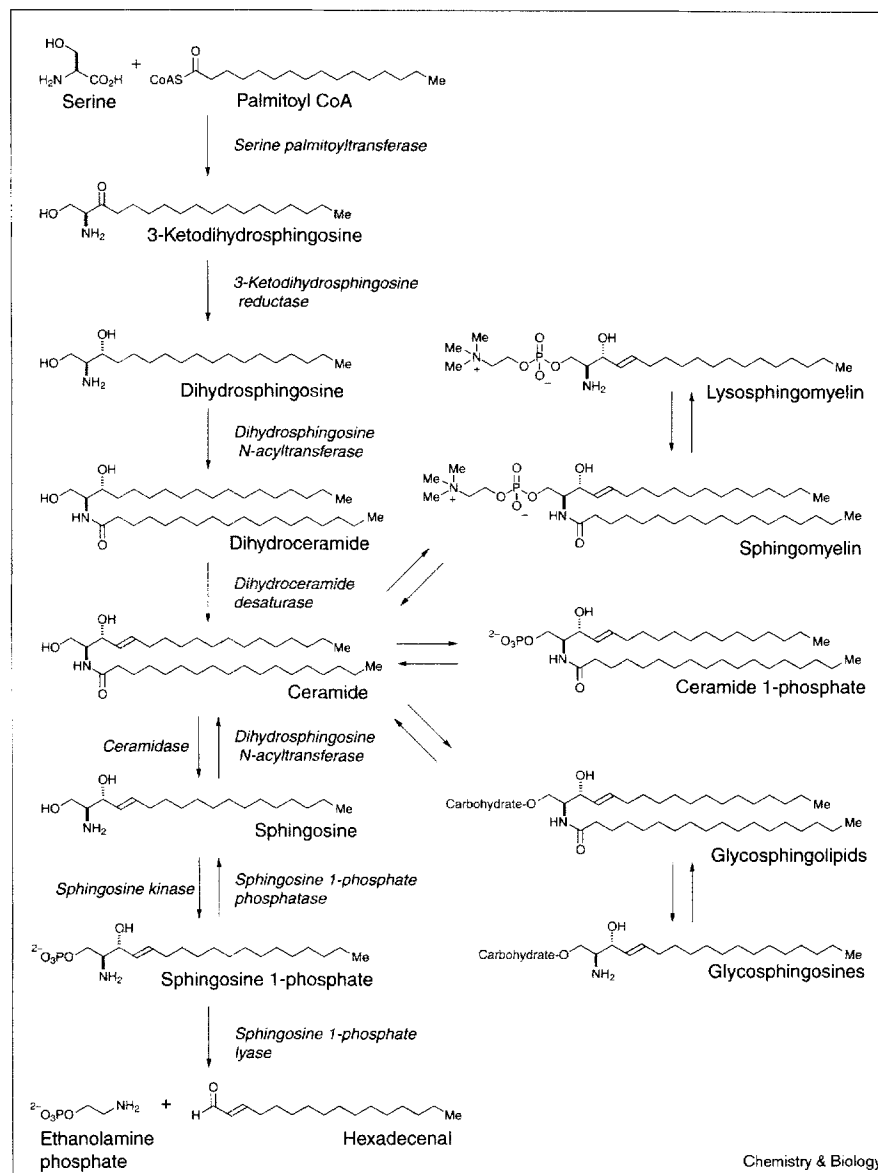
exogenous C2-ceramide can prevent CTLL-2 apoptosis triggered by IL-2 deprivation by inducing  $G_0$  arrest and inhibiting bcl- $X_L$  degradation [18].

These mechanistic ambiguities are exacerbated by the biological properties of myriocin-related compounds. Structural analogs such as 2-alkyl-2-amino-1,3-propanediols, FTY720 (2; Figure 1) and 2-substituted-2-aminoethanols are equipotent to myriocin in MLR and skin-allograft assays but do not inhibit SPT [19,20]. Moreover, a myriocin-like SPT inhibitor, sphingofungin B (3; Figure 1), is sensitive to structural modifications that are known to be inconsequential to the immunosuppressive activity of myriocin, suggesting an SPT-independent mechanism for immune response regulation [21]. Fujita and coworkers [19] have speculated that these synthetic derivatives inhibit downstream sphingolipid biosynthesis enzymes such as dihydrosphingosine *N*-acyltransferase, but additional studies suggest otherwise. Molecules that are structurally related to the immunosuppressive 2-substituted-2-amino-1,3-propanediols or 2-substituted-2-aminoethanols do not inhibit the incorporation of serine into sphingolipids [22,23], and fumonisin B1, a potent inhibitor of dihydrosphingosine *N*-acyltransferase, does not prevent the rescue of myriocin-treated CTLL-2 cells by exogenous sphingosine [9]. These experimental observations argue for two possible scenarios: that myriocin suppresses the immune system by inhibiting SPT in lymphocytes and the myriocin analogs fortuitously target another protein that is necessary for the immune response; or that myriocin itself has two biochemical targets, one related to SPT activity and the other essential for normal immunological activity — and myriocin analogs retain this second activity at the expense of SPT inhibition.

Despite these questions, a systematic appraisal of myriocin-binding proteins has not been accomplished. In principle, such polypeptides could be components of SPT, which has eluded biochemical purification since its discovery in 1967 [10]. Complementation studies of *S. cerevisiae* auxotrophs have identified two genes that encode putative SPT subunits, *LCB1* and *LCB2* [24–26], and mammalian homologs have recently been cloned (Figure 3) [27,28]. Although overexpression studies suggest indirectly that both yeast proteins are essential for SPT activity, similar analyses of the mammalian SPT proteins are contradictory and inconclusive [26–28]. Weiss and Stoffel [27] have reported that coexpression of murine *LCB1* and *LCB2* or overexpression of *LCB2* alone in HEK 293 cells causes a threefold increase in SPT activity compared with untransfected cells, yet HEK 293 cells transfected with only *LCB1* cDNA are unchanged. Furthermore, overexpression of an inactive *LCB2* mutant abolishes SPT activity in HEK 293 cells. These results support a role for mammalian *LCB2* in 3-ketodihydrosphingosine synthesis but leave the functional relevance of *LCB1* in question. In contrast, Hanada

**Figure 2**

The current model of mammalian sphingolipid biosynthesis and catabolism.

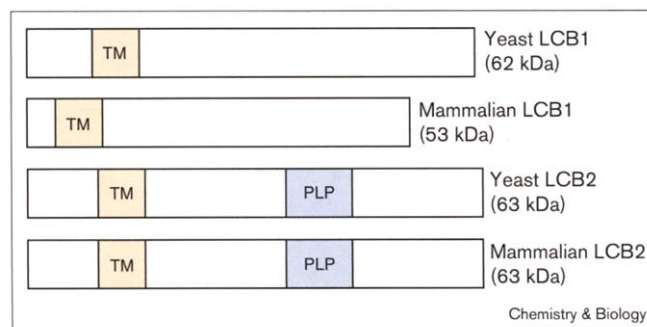


*et al.* [28] have demonstrated that SPB-1 chinese hamster ovary (CHO) cells, a cell line that contains thermolabile SPT, can regain 3-ketodihydrosphingosine synthesis at non-permissive temperatures upon transfection with hamster LCB1 cDNA. The participation of LCB1 in mammalian sphingolipid biosynthesis is also substantiated by the ability of  $\text{Ni}^{2+}$ -immobilized resins to partially sequester microsomal SPT activity from SPB-1 CHO cells overexpressing His<sub>6</sub>-tagged hamster LCB1 protein. The discrepancies between these two studies remain to be resolved, and confirmation of these proteins or other polypeptides as SPT subunits awaits the purification of this elusive enzymatic activity. It is also possible that myriocin targets other cellular proteins that could be direct mediators of

the cellular immune response. This scenario is reasonable because sphingosine-derived molecules often have pleiotropic biological effects. For example, sphingosine 1-phosphate has distinct extracellular and intracellular targets that independently mediate its effects on cell adhesion and cell proliferation [17,29].

To address these issues, we have initiated biochemical studies towards the isolation and characterization of myriocin-binding proteins. Myriocin was obtained from fermentation broths of *M. sterilia*, and previously unknown synthetic derivatives of this natural product were prepared and evaluated in CTLL-2 proliferation and microsomal SPT assays. Guided by these results, myriocin-containing

Figure 3



Schematic representation of the yeast and mammalian LCB proteins. Putative transmembrane (TM) and PLP-binding regions (PLP) are shown.

affinity matrices were then developed, yielding two specific binding proteins from CTLL-2 microsomes. Molecular analyses of these polypeptides using sodium dodecyl sulfate–polyacrylamide gel electrophoresis (SDS–PAGE), LCB1- and LCB2-specific antibodies, and mass spectrometry (MS)-based sequencing conclusively establish that the two proteins are murine LCB1 and LCB2. The implications and limitations of these observations will be discussed.

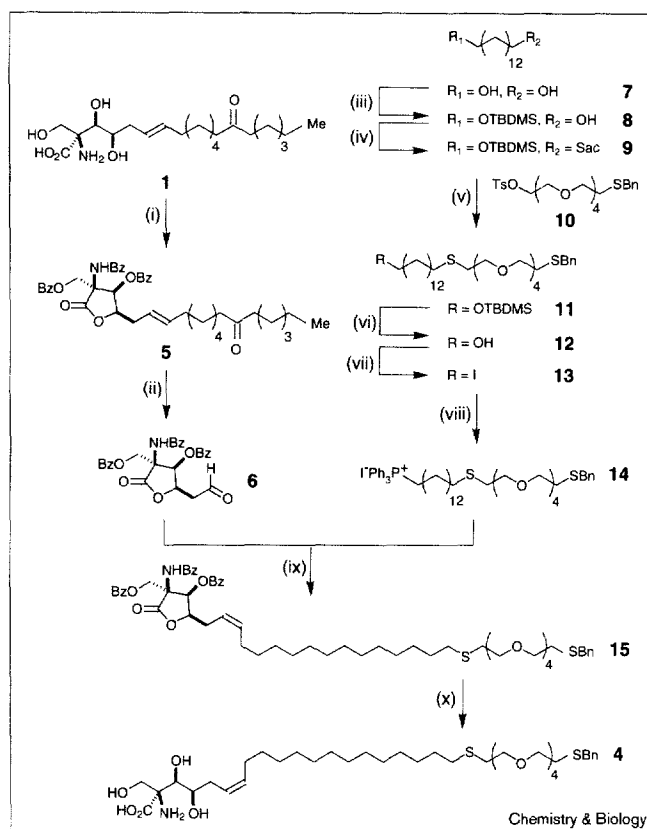
## Results and discussion

### Chemical synthesis of myriocin derivatives

Aliphatic linkers of suitable length and amide-forming transformations have traditionally been used in the preparation of affinity chromatography reagents. The unique chemical and structural properties of myriocin, however, argue against these conventional strategies. Myriocin is highly insoluble in most aqueous or organic solvents; its tail group is very hydrophobic, and its polar head group is densely functionalized. As a result, derivatizing myriocin with an aliphatic chain is likely to yield a ceramide-like compound that is highly intractable to *in vitro* and *in vivo* studies, and acylation reactions might not exhibit sufficient site-selectivity. Such a dialkyl derivative would also be expected to exhibit significant nonspecific binding to cellular proteins, especially when conjugated to a solid support. To circumvent these possible problems, three myriocin-derived compounds were assessed, each containing a pentaethylene glycol linker terminated with a latent thiol functionality.

The first of these compounds is C20-linker myriocin (**4**; Figure 4), which bears its pentaethylene glycol linker at the aliphatic extremity of myriocin. The myriocin portion of this molecular probe deviates from the natural-product structure in two respects: the C14 ketone is removed and the olefin geometry is altered. Incorporated for synthetic simplicity, these structural modifications should have no deleterious effects on biological activity; the E and Z isomers of C14-deoxomyriocin are equipotent to myriocin

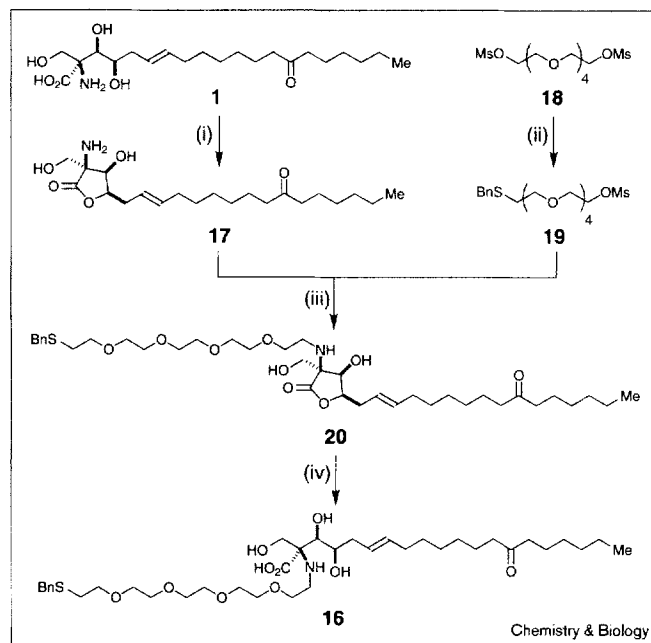
Figure 4



Synthesis of S-benzyl, C20-linker myriocin. (i)  $\text{BzCl}$ , pyr, rt, 74%; (ii)  $\text{O}_3$ ,  $\text{Me}_2\text{S}$ ,  $\text{CH}_2\text{Cl}_2/\text{MeOH}$ ,  $-78^\circ\text{C}$ , 71%; (iii)  $\text{NaH}$ , TBDMSCl, THF, rt, 49%; (iv)  $\text{MsCl}$ ,  $\text{CH}_2\text{Cl}_2$ ,  $0^\circ\text{C}$  then  $\text{KSAc}$ ,  $\text{Et}_2\text{O}$ , rt, 93%; (v)  $\text{KOH(aq)}$ , THF/MeOH, rt, 76%; (vi) TBAF, THF, rt, 94%; (vii)  $\text{I}_2$ ,  $\text{Ph}_3\text{P}$ , imid,  $\text{CH}_3\text{CN}/\text{Et}_2\text{O}$ , rt, 96%; (viii)  $\text{Ph}_3\text{P}$ ,  $\text{CH}_3\text{CN}$ , reflux, 99%; (ix)  $\text{NaN(TMS)}_2$ , THF,  $-78^\circ\text{C}$  to  $0^\circ\text{C}$ , 21%; (x)  $\text{LiOH(aq)}$ , EtOH,  $40^\circ\text{C}$ , 58%.

in murine allogenic MLR assays [30,31]. To synthesize this derivative, myriocin was treated with benzoyl chloride to provide the fully protected lactone (**5**) and then reductively ozonized to generate the labile aldehyde (**6**). A Wittig coupling between the myriocin-derived aldehyde **6** and the ylide obtained from phosphonium iodide **14** then completed the C20-linker myriocin framework, albeit in poor yields. As would be predicted from general *cis/trans* selectivities of nonstabilized ylides, nuclear magnetic resonance (NMR) spectra of the Wittig product (**15**) indicate that only the Z isomer is formed. Benzoyl deprotection and lactone hydrolysis of **15** was finally achieved by LiOH-mediated saponification, yielding the desired myriocin derivative **4**.

Myriocin-based probes that contain modifications of the polar head group were also synthesized for biological evaluation (Figures 5,6). N-linker myriocin (**16**) was prepared by alkylating the myriocin lactone (**17**) with a pentaethylene glycol derivative (**19**). Saponification of the modified lactone (**20**) with LiOH then generated the appropriate

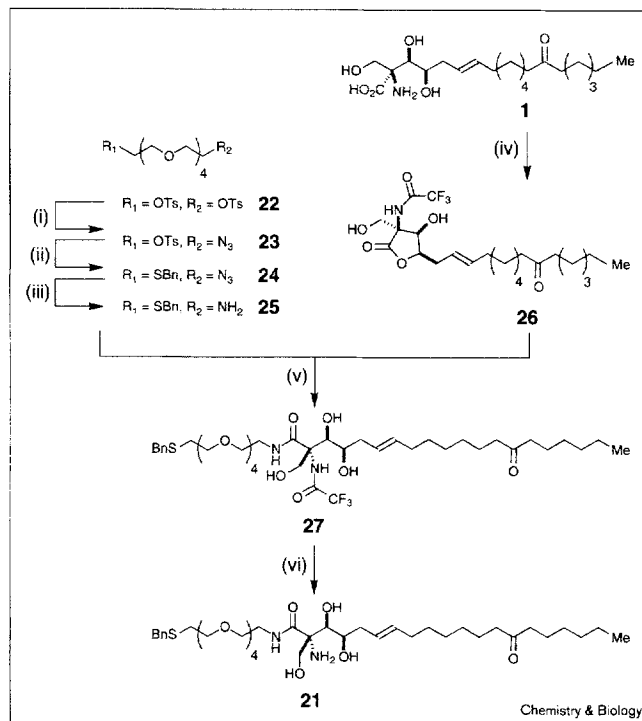
**Figure 5**

Synthesis of *S*-benzyl, *N*-linker myriocin. (i) SOCl<sub>2</sub>, MeOH, -78°C to rt, 81%; (ii) BnSH, Cs<sub>2</sub>CO<sub>3</sub>, EtOH/THF, rt, 22%; (iii) DIPEA, iPrOH, 80°C, 38%; (iv) LiOH (aq), THF/MeOH, rt, 61%.

myriocin derivative **16**, which is functionalized at its amino terminus but contains a basic sp<sup>3</sup>-hybridized nitrogen atom. This structural moiety was intentionally retained because *N*-acetylation of myriocin is known to significantly attenuate its immunosuppressive activity [30]. Design of the third and final myriocin-derived probe, C1-linker myriocin (**21**), was also guided by structure-activity relationship (SAR) data reported by Fujita *et al.* [30]. Construction of this myriocin derivative required the trimethyl aluminum-mediated aminolysis of the *N*-trifluoroacetyl myriocin lactone (**26**) with an amine-functionalized linker (**25**), forming the *N*-acylated myriocin derivative (**27**). Removal of the trifluoroacetyl group with potassium carbonate afforded the final product **21**, which is stable in neutral or acidic conditions but prone to relactonization upon prolonged exposure to base.

#### Biological evaluation of myriocin derivatives

Because Miyake *et al.* [9] have established CTLL-2 cell proliferation as a model system for investigating myriocin activity, we evaluated the effects of **1**, **4**, **16** and **21** on this cell line. Consistent with previous reports [9], myriocin (**1**) inhibits CTLL-2 cell growth with an IC<sub>50</sub> of approximately 10 nM, through the induction of apoptotic pathways (Figure 7). The *N*-linker (**16**) and C1-linker (**21**) compounds demonstrate significant but diminished activity with IC<sub>50</sub> values of approximately 500 and 300 nM, respectively. In contrast, the C20-linker myriocin (**4**) cannot

**Figure 6**

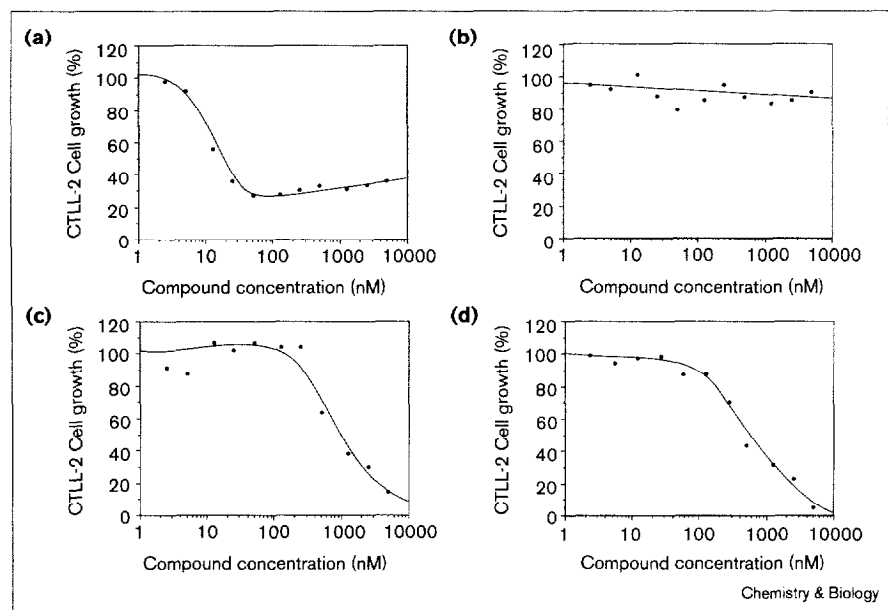
Synthesis of *S*-benzyl, C1-linker myriocin. (i) NaN<sub>3</sub>, DMF, rt, 49%; (ii) BnSH, Cs<sub>2</sub>CO<sub>3</sub>, EtOH/THF, rt, 68%; (iii) NaOH(aq), Ph<sub>3</sub>P, THF, rt, 97%; (iv) TFAA, CH<sub>2</sub>Cl<sub>2</sub>, rt, 100%; (v) AlMe<sub>3</sub>, PhCH<sub>3</sub>/CH<sub>2</sub>Cl<sub>2</sub>, rt, 26%; (vi) K<sub>2</sub>CO<sub>3</sub>, MeOH/H<sub>2</sub>O, rt, 72%.

prevent CTLL-2 proliferation at concentrations up to 5 μM. To confirm further that the *N*- and C1-linker compounds (**16** and **21**) are functionally equivalent to myriocin, both derivatives were then assayed for their ability to inhibit SPT activity in CTLL-2-derived microsomes (Figure 8). Myriocin potently inhibits this process with an IC<sub>50</sub> of 0.28 nM, and both *N*- and C1-linker myriocin have IC<sub>50</sub> values of ~200 nM. C20-linker myriocin (**4**) has no significant effect on SPT activity, even at micromolar concentrations. These results correlate with the antiproliferative activities of myriocin and its derivatives and indicate that the pentaethylene glycol-modified compounds are suitable probes for myriocin-binding proteins. It is noted, however, that *N*- and C1-modifications of myriocin attenuate its ability to abrogate SPT activity more substantially than they affect its ability to induce CTLL-2 apoptosis. This effect might reflect differences in the biophysical properties of myriocin and its derivatives (such as membrane permeability) or the existence of multiple myriocin targets in CTLL-2 cells.

#### Synthesis of myriocin affinity matrices

The preparation of affinity matrices containing the *N*- and C1-linker derivatives was then carried out using cross-linked

Figure 7

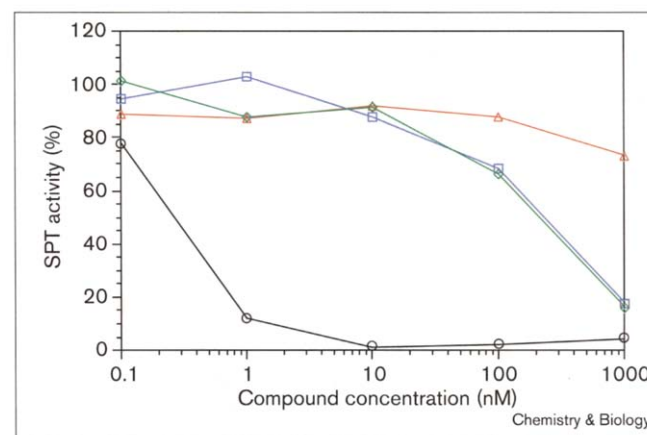


Inhibition of CTLL-2 cell growth by (a) myriocin and its derivatives, (b) C-20 linker myriocin 4, (c) N-linker myriocin 16 and (d) C1-linker myriocin 21.

agarose resins. Our original plan was to liberate the thiol groups in **16** and **21** by metal-ammonia reduction of the benzyl groups. Unfortunately, both sodium- and calcium-mediated deprotections resulted in complex mixtures, and new thiol protecting groups had to be used. The *N*-linker myriocin compound was therefore redesigned as the *S*-acetyl lactone (**28**), using chemical transformations analogous to those used in the synthesis of **20** (Figure 9). LiOH saponification of **28** then provided the *N*-linker myriocin thiol (**29**), which was reacted with ten equivalents of maleimide-functionalized Affigel 102 (**30**). Remaining thiol-reactive groups in the matrix were quenched with an excess of  $\beta$ -mercaptoethanol. Likewise, preparation of the C1-linker myriocin affinity matrix required the development of new carboxyl-functionalized myriocin derivatives. Because of the base sensitivity of C1-linker myriocin, its thiol group was introduced as a trityl thioether for subsequent deprotection by trifluoroacetic acid and trichlylsilane. The C14 carbonyl of myriocin was also reduced to the secondary alcohol with sodium borohydride prior to unmasking the thiol because trityl deprotection in the presence of the ketone yields an macrocyclic hemiketal that is unreactive with the resin-bound maleimide (data not shown). This structural modification should not affect the ability of C1-linker myriocin-containing matrices to sequester binding proteins, because myriocin and C14-hydroxy myriocin are equipotent in MLR assays [30]. Maleimide-functionalized agarose (**30**) was therefore reacted with the C1-linker myriocin thiol and  $\beta$ -mercaptoethanol to provide the second myriocin affinity matrix (**32**; Figure 10), using conditions identical to those for the synthesis of **31**.

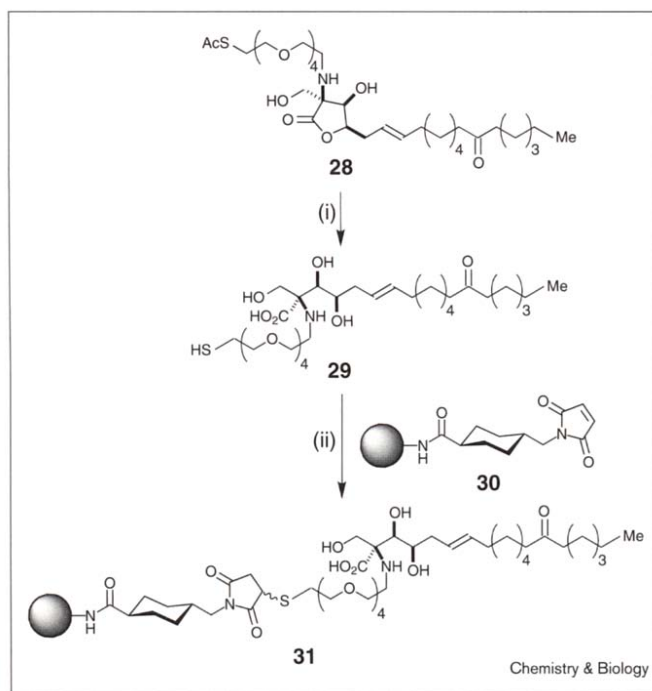
Ultimately, the efficacy of these myriocin affinity matrices depends upon their capacity for specific protein binding from cell lysates. To evaluate the macromolecular accessibility of matrices **31** and **32**, their ability to sequester SPT activity was examined (see Figure 10). The *N*-linker (**31**) and C1-linker (**32**) myriocin matrices were incubated with detergent-solubilized CTLL-2 microsomes and the resultant supernatant was assayed for SPT activity. These experiments clearly demonstrate that the *N*-linker myriocin affinity matrix can deplete cell lysates of the enzymatic activity,

Figure 8



Inhibition of CTLL-2 microsomal serine palmitoyltransferase activity by myriocin (**1**, black circles), C20-linker myriocin (**4**, red triangles), *N*-linker myriocin (**16**, blue squares), and C1-linker myriocin (**21**, green diamonds).



**Figure 9**

Synthesis of *N*-linker myriocin affinity matrix. (i) LiOH(aq), THF/MeOH, 0°C, 60%; (ii) TCEP, MeOH/PBS (pH 7.4), rt, 100%.

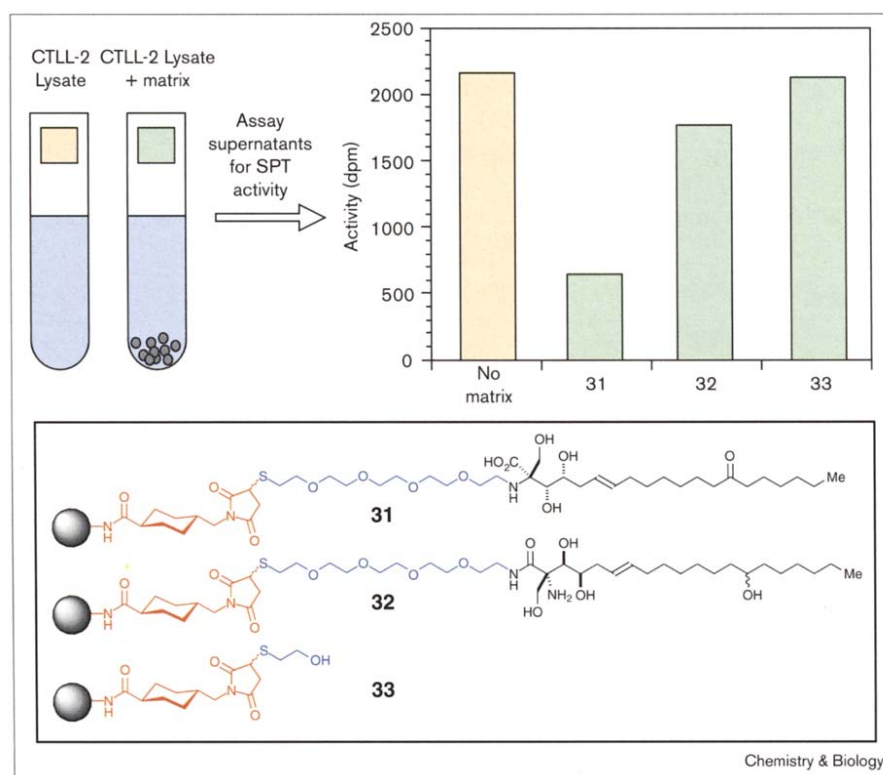
whereas a  $\beta$ -mercaptoethanol-derivatized control matrix (33) does not affect soluble SPT levels. Surprisingly, the C1-linker myriocin matrix has significantly diminished capacity for binding the activity, presumably due to sub-optimal ligand presentation on the agarose support. This hypothesis is substantiated by the ability of both myriocin derivatives to deplete SPT activity from cell lysates when they are conjugated to polydimethylacrylamide beads (data not shown). Guided by these observations, the *N*-linker myriocin matrix (31) was selected for further studies in conjunction with CTLL-2 lysates.

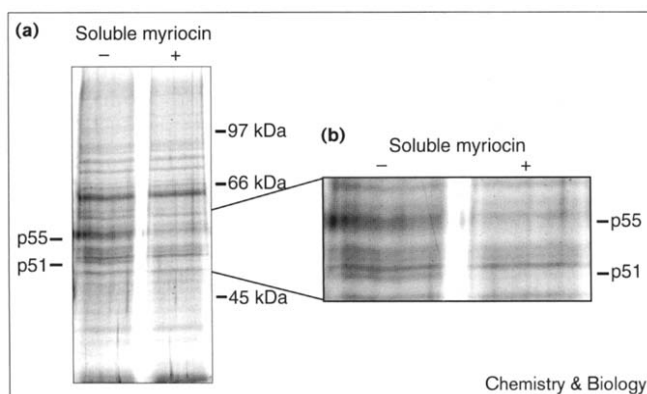
### Isolation and characterization of myriocin-binding proteins in CTLL-2 cells

Subcellular fractions of CTLL-2 lysates were analyzed with the *N*-linker myriocin matrix (31) on an individual basis to identify specific myriocin-binding polypeptides. Differential centrifugation and partial detergent solubilization provided four separate fractions: proteins associated with intact nuclei, mitochondria and lysosomes; microsomal proteins not solubilized by 0.1% IGEPAL CA 630; microsomal proteins solubilized by 0.1% IGEPAL CA 630; and cytosolic proteins. Each subcellular fraction was incubated with 31 (final apparent concentration = 8.1  $\mu$ M) in the presence or absence of soluble myriocin (final concentration = 4.0  $\mu$ M), and, after extensive washing, sequestered proteins were denatured from the myriocin-containing beads

**Figure 10**

Binding of factors comprising serine palmitoyltransferase activity by myriocin-containing matrices.



**Figure 11**

Detergent-solubilized proteins from CTLL-2 microsomes that bind to the *N*-linker myriocin matrix (**31**). **(a)** Complete range of matrix-associated proteins. **(b)** Close-up view of the 50–60 kDa region. Specific myriocin-binding proteins p51 and p55 do not associate with the affinity matrix in the presence of soluble myriocin. (The 60 kDa protein in this gel that appears to be able to compete with myriocin is nonreproducible and was not characterized further).

and separated by SDS-PAGE. Specific myriocin-binding proteins were then identified by the ability of soluble myriocin to abrogate their interactions with the natural-product-displaying affinity matrix.

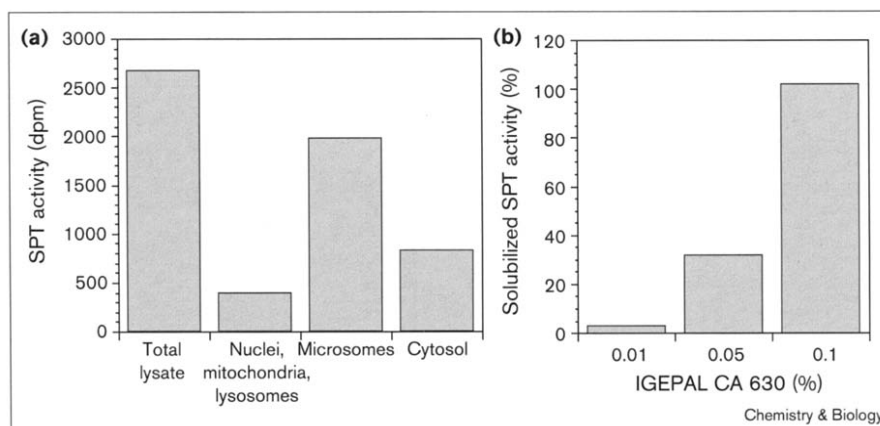
Regardless of the cellular fraction, the vast majority of matrix-associated proteins are nonspecific in nature, consistent with the hydrophobic character of this natural product. Two polypeptides, however, are specific myriocin-binding proteins with apparent molecular weights of 51 and 55 kDa (Figure 11). These proteins, p51 and p55, are predominantly associated with the IGEAL-CA-630-solubilized microsomal fraction, although they also segregate with cytosolic proteins to some degree. This pattern of subcellular localization is reminiscent of previous reports that SPT

activity resides in the endoplasmic reticulum and can be membrane-dissociated with nonionic detergents [27,32]. SPT activities in CTLL-2 subcellular fractions were therefore measured *in vitro*, substantiating this correlation; the highest levels of SPT activity were found in the IGEAL-CA-630-solubilized CTLL-2 microsomes and some residual activity was associated with the cytosol (Figure 12). Given this empirical correspondence and the apparent masses of the myriocin-binding proteins, it seemed likely that the two polypeptides are identical to murine LCB1 and LCB2.

Although the apparent molecular weights of p51 and p55 do not exactly match those calculated for LCB1 (53 kDa) and LCB2 (63 kDa), transcription and translation of LCB1 and LCB2 cDNAs *in vitro* yield products that co-migrate with the two isolated proteins in SDS-PAGE (data not shown). These *in vitro*-translated products should be identical to the endogenous CTLL-2 LCB proteins because previous studies demonstrate that the two putative SPT subunits do not undergo post-translational modifications [27]. Further characterization of p51 and p55 was subsequently conducted through sequencing by ion-trap mass spectrometry (MS). Individual protein bands were excised from SDS-PAGE gels and proteolytically digested in gel with trypsin. The resultant peptides were then fractionated by reverse-phase microcapillary high performance liquid chromatography (HPLC) and subjected to MS fragmentation and analysis, producing spectra for sequence interpretation and database correlation [33,34]. The isolated p51 protein yielded a peptide fragment corresponding to murine LCB1 (VVVTVEQTEELQR, residues 446–459) along with a few peptides from isobaric proteins, and the p55 protein afforded several fragments of LCB2 (SSTATVAAAGQIHVTENGGLYK, residues 32–54; HNNMQSLEK, residues 280–288; NIGVVVGFPAITPIESR, residues 488–505; EIDEVGDLLQLK, residues 525–536; and LVPLLDPRPFDETTEETED, residues 542–560). These results indicate that the SDS-PAGE

**Figure 12**

Subcellular localization of serine palmitoyltransferase activity (SPT). **(a)** SPT activity in various lysate fractions obtained by differential centrifugation. **(b)** Solubilization of microsomal SPT activity by IGEAL CA 630.





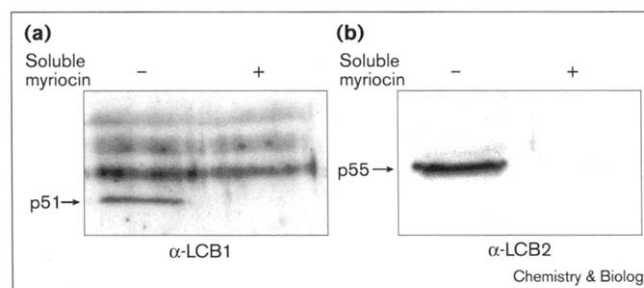
bands corresponding to p51 and p55 contain the putative SPT subunits and therefore LCB1 and LCB2 associate with the *N*-linker myriocin matrix (31). Due to the non-quantitative character of MS and the abundance of non-specific binding proteins, it is difficult to ascertain from these data alone whether LCB1 and LCB2 are the primary constituents of the p51 and p55 bands, respectively. The relative scarcity of LCB1-derived peptides could be due to inherent chemical properties of LCB1 that impede its proteolysis or mass spectrometry analysis.

Final confirmation that p51 is murine LCB1 and p55 is murine LCB2 was obtained by western-blot analyses of matrix-associated proteins (Figure 13). Specific polyclonal antibodies were generated against unique carboxy-terminal regions of LCB1 (STGSREKDVKLLQAI, residues 401–415) and LCB2 (KYSRHRLVPLLDLPF, residues 536–550) and used to probe affinity-matrix-bound proteins that were separated by SDS-PAGE and transferred to a PDVF membrane. The  $\alpha$ -LCB1 antibody clearly recognizes a 51 kDa protein that binds 31 in the absence but not presence of soluble myriocin. Similarly, the  $\alpha$ -LCB2 antibody recognizes a 55 kDa protein that specifically associates with 31. Neither protein could be detected with preimmune sera, verifying the selective nature of the antibody–protein interactions. In conjunction with the co-migration and MS-based sequencing experiments, these tests conclusively demonstrate that LCB1 and LCB2 are specific myriocin-binding proteins in CTLL-2 microsomes.

#### Biological implications and experimental limitations

The identification of LCB1 and LCB2 as myriocin-binding proteins corroborates previous observations that myriocin inhibits sphingolipid biosynthesis [8,9], and constitutes the first demonstration that myriocin acts directly on SPT-related proteins. Most importantly, it provides a biochemical link between SPT activity and the two subunits, which were originally identified as putative SPT subunits in yeast genetic screens. The potent myriocin-mediated inhibition of SPT *in vitro*, the ability of myriocin-containing beads to deplete SPT activity from CTLL-2 lysates, and the specific isolation of endogenous LCB1 and LCB2 by these matrices testifies that both LCB proteins are integral components of mammalian SPT, contrary to previous suppositions [27]. The exclusive observation of LCB1 and LCB2 as specific myriocin-binding proteins shows for the first time that the two subunits are directly responsible for SPT activity and are not merely upstream regulators of 3-ketodihydrosphingosine biosynthesis. Nagiec *et al.* [26] have noted that LCB1- and LCB2-related proteins such as 2-amino-3-ketobutyrate CoA ligase, 8-amino-7-oxononanoate synthase, and 5-aminolevulinic acid synthase are pyridoxal 5'-phosphate (PLP)-using homodimeric enzymes that catalyze the  $\alpha$ -carbon acylation of various amino acids. It therefore seems likely that LCB1 and LCB2 heterodimerize to maintain and regulate SPT activity. Alternatively, the LCB proteins

**Figure 13**

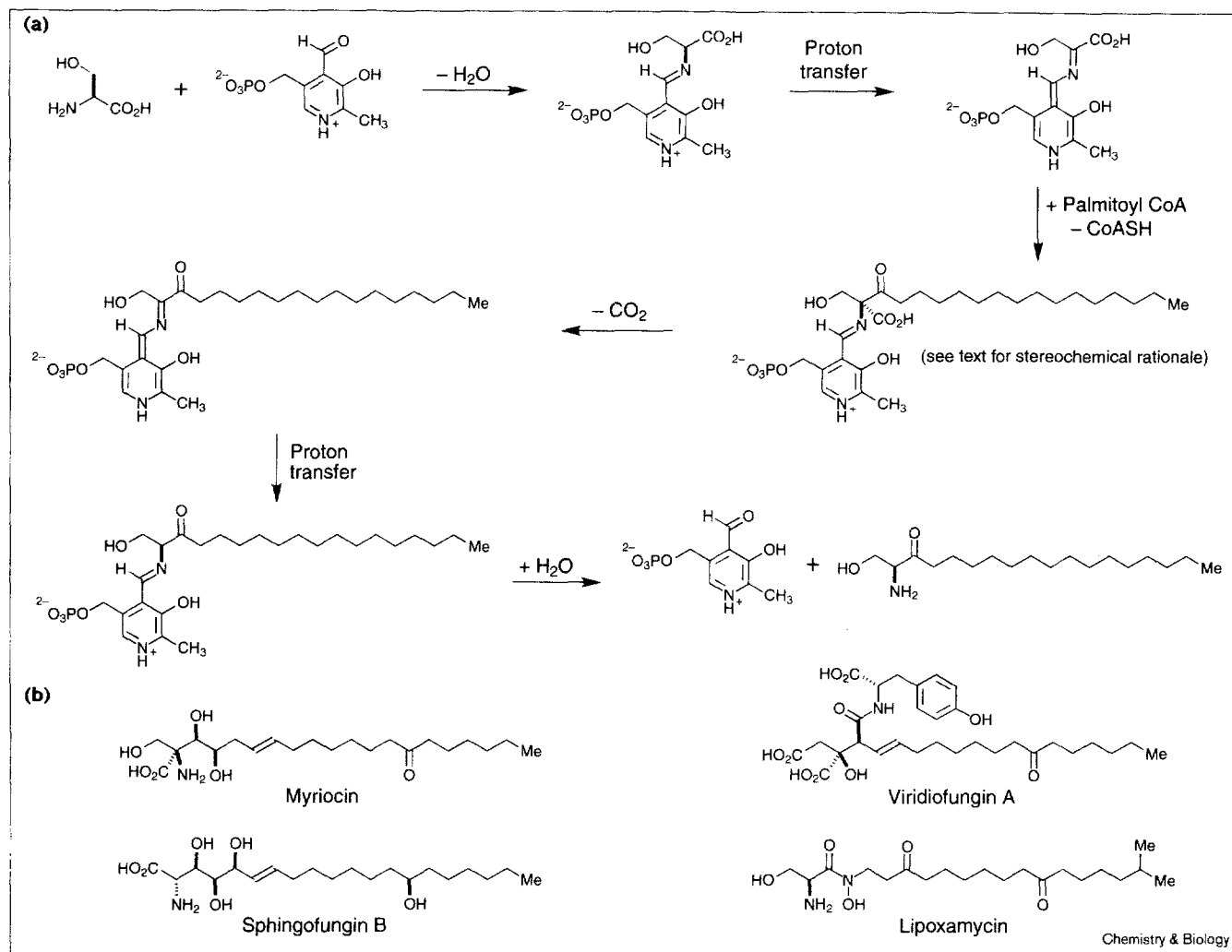


Western blot analyses of affinity matrix-associated proteins. **(a)** Recognition of specific myriocin-binding protein p51 by an  $\alpha$ -LCB1 antibody. Cross-reactive proteins bind to the matrix nonspecifically and are also recognized by preimmune sera (data not shown). **(b)** Recognition of specific myriocin-binding protein p55 by an  $\alpha$ -LCB2 antibody. Neither p51 or p55 is recognized by preimmune sera.

could contribute independently to SPT activity by homodimerization, but the absence of a complete PLP-binding site in LCB1 argues against this model. In any case, the existence of other catalytic or regulatory SPT components cannot be ruled out even though none was observed in these experiments; myriocin might abrogate 3-ketodihydrosphingosine synthesis by binding a subset of SPT components or by disrupting a larger complex. It is also possible that the affinity chromatography conditions (0.1% detergent, 250 mM NaCl) partially dissociate a larger SPT complex, although SPT retains optimum activity levels in this buffer medium (data not shown).

Consistent with these observations, the ability of myriocin to inhibit SPT is remarkably congruent with the currently accepted mechanism of 3-ketodihydrosphingosine biosynthesis (Figure 14). Isotopic-labeling studies suggest that the reaction proceeds by sequential imine formation,  $\alpha$ -carbon deprotonation, palmitoylation, decarboxylation, protonation and imine hydrolysis [35]. (This mechanism is in contrast with an otherwise reasonable alternative of imine formation, decarboxylation, palmitoylation and hydrolysis). The observation that serine decarboxylation is palmitoyl CoA-dependent provides additional support for this mechanism and indicates the importance of a C3-ketone for substrate decarboxylation [36]. Furthermore, the conservation of C2-configuration in serine and 3-ketodihydrosphingosine demands that the  $\alpha$ -proton/palmitoyl CoA and carboxyl group/proton substitutions proceed by a combination of stereochemical inversion and retention. Within this context, it is likely that the first transformation occurs with inversion of configuration and the second with retention because this sequence would require the least molecular motion in the enzyme–substrate complex. This mechanistic course is also more consistent with the structure of myriocin; the natural product stereochemically matches the putative reaction intermediate preceding decarboxylation (see Figure 14),

Figure 14



Serine palmitoyltransferase activity and its molecular inhibition. (a) The currently accepted mechanism for 3-ketodihydrosphingosine biosynthesis. (b) Known SPT inhibitors.

and the lack of a C3-keto group in myriocin provides a plausible basis for its potent inhibitory activity. The absence of this group should prevent the enzyme from decarboxylating the inhibitor. Other known SPT blockers such as lipoxamycin, the sphingofungins and the viridifungins are structurally divergent from this molecular intermediate, and accordingly they are weaker inhibitors of sphingolipid biosynthesis than myriocin. It remains to be shown, however, that myriocin truly abrogates SPT activity by substrate-competitive binding. Miyake *et al.* [9] have reported that myriocin inhibits SPT noncompetitively with respect to palmitoyl CoA, whereas it has been claimed that the sphingofungins compete with serine in SPT assays [37].

In any case, SPT deactivation is biochemically consistent with the effect of myriocin on CTLL-2 proliferation and apoptosis, because sphingolipids are known modulators of

both cellular processes [38,39]. The addition of sphingosine and sphingosine 1-phosphate to mammalian fibroblasts can stimulate DNA synthesis and cell proliferation [40,41], and the carcinogenic dihydrosphingosine *N*-acyltransferase inhibitor fumonisin B1 is believed to stimulate fibroblast mitogenesis by causing intracellular sphingoid base accumulation [42]. Cellular targets of such sphingolipids are still enigmatic, but both sphingosine and sphingosine 1-phosphate can modulate intracellular calcium mobilization and specific growth-promoting protein kinases [15,41,43,44]. These observations suggest that the intracellular depletion of certain sphingolipids could impede cell growth or survival.

It is important to recognize, however, that sphingolipids have multiple effects, many of which may be cell lineage-dependent. In addition to their mitogenic influence on

Swiss 3T3 fibroblasts, sphingosine and sphingosine 1-phosphate can induce apoptosis in several cell lines [45–47] and the SPT inhibitor  $\beta$ -fluoroalanine has no effect on fibroblast proliferation [42]. Moreover, fumonisins B1-induced accumulation of sphingobases activates apoptotic pathways in colon-derived HT29 cells [48]. Interpretation of these seemingly conflicting observations is further complicated by the dynamic nature of sphingolipid homeostasis, maintained by the rapid metabolic conversion of exogenous sphingolipids by intracellular enzymes. What remains clear is that cell survival and proliferation are intimately connected to specific sphingolipid compositions and concentrations. The specific outcome of sphingolipid depletion or accumulation depends on the cell type and the influence of exogenous factors. Because myriocin has no effect on the proliferation of several tumor cell lines of diverse origin [3,7], it is conceivable that myriocin specifically promotes programmed cell death in CTLL-2-like cells, thereby suppressing the immune response against transplanted cells and tissue grafts. Nakamura *et al.* [7] have suggested that myriocin sensitivity is limited to CD4-negative and CD8-positive cytotoxic T cell lineages, although the myriocin-induced apoptosis of cerebellar Purkinje neurons has recently been demonstrated [49].

Whether SPT deactivation is the primary mechanism for myriocin-mediated immunosuppression is a more difficult question to answer, due to the multifaceted nature of the mammalian immune system. The inability of FTY720 and other myriocin-derived immunosuppressants to inhibit sphingolipid biosynthesis implies either a fortuitous divergence in physiological mechanism or the existence of another biological target for myriocin. The latter scenario would not be unprecedented because sphingoid bases often have multiple cellular effects and presumably interact with several proteins. Sphingosine 1-phosphate has recently emerged as the prototype for such multifunctional sphingolipids. At the intracellular level, this sphingosine metabolite can induce mitogenesis and suppress apoptosis [38], but it also binds cell-surface receptors such as endothelial differentiation gene-1 (EDG-1) to induce cadherin upregulation and cell–cell aggregation [29]. These diverse cellular phenotypes are mechanistically distinct, demonstrating the presence of at least two protein receptors for this novel sphingolipid [17]. FTY720 itself appears to have two discrete effects; the immunosuppressive agent can specifically induce the apoptosis of rat spleen cells and human peripheral blood cells, but at lower concentrations it accelerates lymphocyte homing and decreases T-cell infiltration of tissue allografts [50–52].

It is even possible that a myriocin (or FTY720) metabolite is the primary mediator of immunosuppressive activity. Some of the sphingolipid biosynthetic enzymes are known to have relatively broad substrate specificities and can act upon numerous exogenous sphingoid bases. Dihydrosphingosine

*N*-acyltransferase can condense all four sphinganine and sphingosine stereoisomers with a variety of fatty acyl-CoAs [53,54], and several sphingoid bases, including all dihydrosphingosine stereoisomers, are phosphorylated *in vivo* by one or more kinases [53,55–57]. Because the degradation of sphingosine-like molecules by sphingosine 1-phosphate lyase appears to be limited to D-erythrosphingoid bases of various chain lengths and types [53,55], these unconventional metabolites might accumulate in cells and induce abnormal phenotypes. In agreement with these observations, the enzymatic conversion of exogenous sphingosine-like molecules into biologically active metabolites is preceded for both acylation and phosphorylation processes [57,58]. Given the related structures of myriocin and FTY720, these sphingosine-like compounds might undergo similar chemical transformations in mammalian cells, possibly generating additional modulatory ligands for essential cellular proteins.

Exploring these possibilities will be a daunting task, requiring the isolation of small molecules and their protein receptors from several tissues or cell types. The molecular studies of myriocin and its derivatives described here therefore represent an initial step forward in the systematic elucidation of their physiological targets. The chemical synthesis of a myriocin-containing affinity matrix has led to the biochemical isolation of LCB1 and LCB2 from CTLL-2 cells, corroborating previous observations that myriocin potently inhibits SPT activity and providing strong experimental evidence that LCB1 and LCB2 are fundamental components of this biosynthetic enzyme. This molecular reagent and others described above might therefore facilitate the discovery of additional myriocin-sensitive proteins, which could be specifically expressed in other tissues or cell lines. As demonstrated by the successful identification of LCB1 and LCB2 as myriocin-binding proteins, these chemistry-based strategies can convey a molecular clarity to biological processes, thereby complementing and supporting traditional genetic approaches.

Alternatively, cDNA and oligonucleotide microarray technologies, which allow the rapid profiling of cellular mRNA transcript levels, could facilitate the mechanistic deconvolution of myriocin's biological activities. The observed sensitivity of *S. cerevisiae* to myriocin and our comprehensive knowledge of the yeast genome sets the stage for several initial experiments. For example, the effects of myriocin and other SPT inhibitors on *S. cerevisiae* mRNA transcripts could be evaluated in order to determine whether myriocin targets yeast proteins that are unrelated to SPT activity. Similar assessments could be obtained by comparing the transcript profiles of yeast mutants lacking LCB1 and/or LCB2 genes to those of myriocin-treated wild-type strains. Microarray technologies would also permit the molecular dissection of SPT-related phenotypes that result from myriocin treatment. Individual contributions of sphingolipid

metabolites to cellular homeostasis could be studied by analyzing yeast mRNA transcript profiles induced by simultaneous exposure to myriocin and specific sphingolipids. These investigations could ultimately be extended to mammalian cell lines, promoting our understanding of myriocin-induced perturbations in multicellular systems. Thus, the combination of small-molecule-based approaches with cDNA/oligonucleotide microarray technologies might constitute a general strategy for the mechanistic evaluation of biologically active compounds. Such investigations are now underway (J. Hardwick, J. Tong, J.K.C. and S.L.S., unpublished observations).

## Significance

The natural product myriocin induces apoptosis of a murine cytotoxic T lymphocyte cell line (CTLL-2) and inhibits a serine palmitoyltransferase (SPT) activity thought to initiate sphingolipid biosynthesis. Using synthetic myriocin derivatives and affinity chromatography, two specific myriocin-binding proteins were isolated from CTLL-2 cell lysates. This study provides the first biochemical evidence that LCB1 and LCB2, mammalian homologs of two yeast proteins that have been linked to sphingolipid biosynthesis, are integral components of SPT, a sphingolipid biosynthesis enzyme that has eluded purification since its discovery three decades ago. Our results also demonstrate that myriocin acts directly upon these protein subunits, thereby inhibiting SPT activity. These results verify the utility of sphingolipid-derived reagents to elucidate the molecular machinery of sphingolipid homeostasis.

## Materials and methods

### *Myriocin isolation from Mycelia sterilia*

*Mycelia sterilia* was obtained from the American Type Culture Collection (ATCC; Rockville, MD) as an agar-slant culture, and all fermentations were performed using autoclaved fermentation media (3% glucose, 0.5% Difco yeast extract, 0.03%  $K_2HPO_4$ , 0.03%  $KH_2PO_4$ , 0.05%  $MgSO_4$ ) and a 37°C shaker incubator (250 rpm). The ATCC agar slant was used to inoculate 3 ml of media, and the fungal culture was maintained for 2 days. The 3 ml culture was then added to 100 ml of media, fermented for another 2 days, and then expanded to a final media volume of 1.1 l. After this 1.1 l culture was incubated for 15 days, the mycelial cake was isolated by filtration, washed with water ( $2 \times 75$  ml), and extracted with methanol ( $4 \times 75$  ml). The methanol extract was subsequently concentrated *in vacuo*, diluted with an equal volume of water, and applied to a 100 ml column of Amberlite XAD-16 (prewashed with five volumes of methanol and five volumes of water; Sigma, St. Louis, MO). The hydrophobic matrix was washed with water ( $5 \times 100$  ml), acetone:water: $NH_4OH$  (1:4:0.02;  $2 \times 100$  ml), and methanol:water (1:1;  $2 \times 100$  ml). Myriocin was finally eluted from the column in methanol:water (4:1;  $50 \times 25$  ml fractions). Myriocin-containing fractions were pooled and solvent was removed *in vacuo* to yield 100–200 mg of crude myriocin (1; at least 90% purity). This crude preparation was used directly in the syntheses of myriocin derivatives or recrystallized from methanol to provide pure myriocin for biological studies.

### *Evaluation of myriocin derivatives in CTLL-2 proliferation assay*

CTLL-2 cells were grown in cell culture media (RPMI 1640; 10% fetal bovine serum, 20 mM HEPES, pH 7.4, 2 mM glutamine, 1 mM sodium pyruvate, 50  $\mu$ M  $\beta$ -mercaptoethanol, 100 U/ml penicillin G, 100  $\mu$ g/ml

streptomycin sulfate, 20 U/ml IL-2) in a 5%  $CO_2$  and 37°C incubator. Myriocin and its derivatives were maintained as 1 mM, 100  $\mu$ M, 10  $\mu$ M and 1  $\mu$ M stocks in methanol and stored at –20°C. Using these reagents, a series of 0.5 ml cultures were established in a 12-well cell culture dish, each containing 25,000 CTLL-2 cells, 1% methanol, and the appropriate myriocin-derived compound at concentrations ranging from 2.5 nM to 5  $\mu$ M. A well containing only CTLL-2 cells and 1% methanol was also included as a control. The cell cultures were maintained for 3 days and then cell populations in each well were counted with either a Levy hemocytometer (Hausser Scientific) or a Coulter Z1 cell counter (particle size range  $\geq 10$  microns; Coulter Electronics).

### *Subcellular fractionation of CTLL-2 cells*

CTLL-2 cells (1 l culture) were grown to a density of approximately 500,000 cells/ml and collected by centrifugation at 200 g for 5 min. The cells were washed once with RPMI 1640 media (40 ml), pelleted again by centrifugation, and resuspended in lysis buffer (50 mM sodium phosphate, pH 7.4, 20% glycerol, 150 mM NaCl, 2 mM EDTA, 2 mM EGTA, 25 mM NaF, 25 mM  $\beta$ -glycerophosphate, 2 mM DTT, 1  $\mu$ M  $Na_3VO_4$ , 1 mM Pefabloc SC (Boehringer Mannheim), 1  $\mu$ g/ml leupeptin, 1  $\mu$ g/ml pepstatin A) to a density of  $3.2 \times 10^7$  cells/ml. All subsequent steps were performed at 4°C. The CTLL-2 cells were first lysed by sonication using a Fisher Scientific Model 550 Sonic dismembrator equipped with a 0.125 in microtip (12 cycles; 10 s sonication/1 min pause). This lysate was centrifuged at 15,000 g for 20 min to yield a pellet, which was subsequently resuspended in lysis buffer (15.6 ml) by sonication (3 cycles; 10 s sonication/1 min pause). The 15,000 g supernatant was recentrifuged at 100,000 g for 1 h to provide the cytosolic supernatant and the microsomal pellet, which was resuspended in lysis buffer (15.6 ml) by sonication ( $3 \times 10$  s sonication/1 min pause bursts). All three subcellular fractions were flash frozen as 1 ml aliquots and stored at –78°C. Further fractionation of the microsomal lysate was typically performed immediately prior to use. The lysate was rapidly thawed and then treated with IGEAL CA 630 (final concentration = 0.1%) for 1 h. The detergent-solubilized mixture was centrifuged again at 100,000 g for 1 h, affording a membranous pellet and a supernatant containing membrane-dissociated proteins. This second 100,000 g pellet was resuspended in lysis buffer (volume equal to the original microsomal lysate volume) by sonication (3 cycles; 10 s sonication/1 min pause).

### *SPT assay and evaluation of myriocin derivatives*

SPT activity in CTLL-2 subcellular fractions was assessed by mixing lysate (40  $\mu$ l) with reaction buffer (50  $\mu$ l: 100 mM HEPES, pH 8.3, 5 mM DTT, 2.5 mM EDTA, 50  $\mu$ M PLP, 150  $\mu$ M palmitoyl CoA) and radioactive serine (10  $\mu$ l; 100 mM stock of  $HOCT_2CH(NH_2)COOH$  from DuPont NEN diluted with nonradioactive serine to a final specific activity of 45,000 dpm/nmol). Each 100  $\mu$ l reaction was incubated at 35°C for 30 min and then quenched with 0.5 N  $NH_4OH$  (1 ml). Organic-soluble radioactive products were isolated by adding 25  $\mu$ g of dihydrosphingosine or sphingosine (1 mg/ml in EtOH) and 0.75 ml of chloroform:methanol (1:2) to the reaction mixture. The biphasic mixture was vortexed vigorously and centrifuged (16,000 g for 2 min), and the resultant aqueous layer was discarded. The organic layer was subsequently washed with water ( $2 \times 1$  ml) by sequential vortexing, centrifugation, and aqueous layer removal, and a 100  $\mu$ l aliquot of the organic layer was mixed with Ecoscint A (3 ml; National Diagnostics) for analysis by a Beckman LS 6500 scintillation counter. The effect of myriocin or its derivatives on SPT activity was determined by using CTLL-2 microsomal lysates (without detergent solubilization) and adding 1  $\mu$ l of either methanol or serial dilutions of the appropriate compound dissolved in methanol (100  $\mu$ M, 10  $\mu$ M, 1  $\mu$ M, 0.1  $\mu$ M or 0.01  $\mu$ M stocks).

### *Synthesis and evaluation of myriocin-affinity matrices*

To prepare the myriocin-affinity matrices, Affigel 102 (5 ml, 81.4  $\mu$ mol of amine; BioRad) was first washed with DMF (5  $\times$  5 ml) and resuspended in a solution of DMF (2.5 ml) containing succinimidyl 4-(*N*-maleimido-methyl)cyclohexane-1-carboxylate (SMCC, Pierce; 40.8 mg, 122  $\mu$ mol) and DIPEA (21.5  $\mu$ l, 122  $\mu$ mol) using a fritted reaction vessel (PD-10 columns, Pharmacia). This suspension was constantly mixed using a

rotating tube shaker for 3 h at room temperature and then drained. The resultant resin derivative was sequentially washed with DMF (5 × 5 ml), isopropanol (5 × 5 ml), and degassed PBS (pH 7.4)/methanol (1:1; 5 × 5 ml). The SMCC-functionalized Affigel (**30**) was then resuspended in degassed PBS (pH 7.4)/methanol (total resin and solvent volume = 5 ml). No free amine remained in the beads, as determined by ninhydrin tests. This procedure generates a maleimide-functionalized agarose matrix, which can then be reacted with either *N*-linker myriocin thiol **29**, or C1-linker myriocin thiol.

A typical matrix synthesis is as follows. *N*-linker myriocin **29** (3.71 mg, 5.82 μmol) and triscarboxyethylphosphine (TCEP; 3.32 mg, 11.6 μmol) were dissolved in degassed methanol:water (4:1; 250 μl) and stirred for 5 min at room temperature. The SMCC-Affigel suspension described above (3.57 ml, 58.2 μmoles) was then added to the myriocin/TCEP solution, and the reaction was incubated on a rotating tube shaker for 18 h at room temperature. Afterwards, an aliquot of the reaction supernatant (15 μl, containing no agarose beads) was analyzed by reverse-phase HPLC (LDC Analytical gradient system; YMC C-18 column, 4.6 mm × 15 cm; linear gradient from 20% to 80% acetonitrile in water containing 0.1% TFA in 25 min) to confirm the complete depletion of **29**, implying quantitative ligand conjugation. Conjugation of myriocin to the agarose was also corroborated by positive ninhydrin tests. The remaining maleimides were quenched by adding β-mercaptoethanol (20.4 μl, 0.291 mmol) to the reaction mixture and incubating the suspension on a rotating tube shaker for 6 h at room temperature. The *N*-linker myriocin-functionalized Affigel (**31**) was then washed with water (5 × 5 ml), methanol (5 × 5 ml), and isopropanol (5 × 5 ml) and finally resuspended in isopropanol (total resin and solvent volume = 7.14 ml). Affigel matrices containing C1-linker myriocin (**32**) were synthesized from **30** and C1-linker myriocin thiol using identical procedures, and the Affigel control matrix (**33**) was prepared by reacting the **30** with β-mercaptoethanol (5 equiv) for 24 h at room temperature. Similar methods were also utilized to conjugate myriocin derivatives and β-mercaptoethanol to ethylaminodiamine-functionalized polydimethylacrylamide (PDMA) beads (Polymer Labs). All synthesized matrices were stored at -20°C.

To evaluate the ability of functionalized Affigel matrices **31**, **32** and **33** to sequester cellular proteins, each resin (10 μl of isopropanol suspension) was washed with water (1 ml) and incubated with CTLL-2 microsomal lysate (200 μl; see above) containing 0.01% IGEPAL CA 630 detergent in a 1.5 ml Eppendorf tube. The mixtures were incubated on a rotating tube shaker for 1 h at 4°C, and then quickly centrifuged to pellet the matrices. Supernatants were subsequently analyzed for SPT activity using the procedures outlined above. Related protocols were followed for the evaluation of myriocin- and β-mercaptoethanol-functionalized PDMA resins.

#### Identification of p51 and p55 by affinity chromatography

In a typical analytical-scale operation, fractionated CTLL-2 lysate (4 ml) was treated with IGEPAL CA 630 (final concentration = 0.1%) and NaCl (final concentration = 250 mM) and then mixed with affinity chromatography buffer (16 ml: 50 mM sodium phosphate, pH 7.4; 20% glycerol; 250 mM NaCl, 0.1% IGEPAL CA 630, 2 mM EDTA, 2 mM EGTA, 25 mM NaF, 25 mM β-glycerophosphate, 2 mM DTT, 1 μM Na<sub>3</sub>VO<sub>4</sub>, 1 mM Pefabloc SC (Boehringer Mannheim), 1 μg/ml leupeptin, 1 μg/ml pepstatin A). The resultant mixture was split into two equal portions (2 × 10 ml), and all subsequent procedures were performed at 4°C. One portion was treated with methanol (20 μl), and the other was treated with myriocin (20 μl of a 2.00 mM solution in methanol). After both portions were equilibrated for 10 min, each was mixed with *N*-linker myriocin affinity matrix (**31**; 100 μl of isopropanol suspension, drained and washed with water (2 × 1 ml) and incubated on a rotating tube shaker for 2 h at 4°C. The two suspensions were then centrifuged at 2000 g for 5 min to pellet the matrices, and the beads were transferred separately to two 2.0 ml Eppendorf tubes. Using these tubes, each matrix was washed with the affinity chromatography buffer (3 × 1 ml; plus 0.2% methanol or 2 μM myriocin, depending on the matrix) and 50 mM sodium phosphate buffer (pH 7.4; 2 × 1 ml) by sequential vortexing, centrifugation, and

buffer removal. Matrix-associated proteins were then recovered by boiling the beads with 2× SDS-PAGE loading buffer (30 μl/aliquot: 100 mM Tris-HCl, pH 6.8; 20% glycerol; 4% SDS; 5% β-mercaptoethanol; 0.2% bromophenol blue) for 5 min. The eluted proteins were separated using standard SDS-PAGE protocols on a 7.5% acrylamide gel and visualized by conventional silver staining procedures. Specific binding proteins p51 and p55 were identified by comparisons between the methanol- and myriocin-treated lysates.

Isolation of specific myriocin-binding proteins for sequencing analysis required a 20-fold increase in scale, using procedures similar to those described above. Matrix proteins were recovered as before by boiling the beads with SDS-containing buffer (50 mM Tris-HCl, pH 6.8, 0.5% SDS, 5% β-mercaptoethanol) for 5 min, and the resin eluates obtained from the methanol-treated lysates were pooled. Both protein solutions were passed through 0.45 μm filters (Millipore Ultrafree) to remove any particulates. Concentration of the methanol-treated eluate was then achieved by first diluting the pooled solution fivefold with buffer (50 mM Tris-HCl (pH 6.8) and 5% β-mercaptoethanol) and cooling it on ice for 30 min. These conditions bring the SDS levels below its critical micelle concentration, allowing the solution volume to be reduced by ultrafiltration (Millipore Ultrafree 4, 10 kD molecular weight cut-off) without excessive SDS concentration. Using this procedure, the methanol-treated eluate were reduced to a volume of 30 μl and then boiled with 5× SDS-PAGE loading buffer (7.5 μl: 60 mM Tris-HCl pH 6.8, 25% glycerol, 2% SDS, 5% β-mercaptoethanol, 0.1% bromophenol blue). The matrix-eluted proteins were separated using standard SDS-PAGE protocols on a 7.5% acrylamide gel and were visualized using a modified silver staining protocol designed for mass spectrometry samples. Bands corresponding to p51 and p55 were identified using a control sample obtained from the myriocin-treated lysates, and excised from the acrylamide gel. The gel fragments were subsequently transferred to separate Eppendorf tubes, washed with acetonitrile:water (1:1; 3 × 1 ml, 1 min each wash), and stored at -20°C until trypsinization and MS-based sequence analysis was performed.

#### PCR cloning of LCB1 and LCB2 cDNAs

**LCB1 cDNA.** The LCB1 cDNA flanked by *Clal* and *EcoRI* restriction sites and a 5' Kozak sequence was PCR-amplified from a mouse adult BALB/c male kidney cDNA library (Clontech QUICK-Clone) using the following primers: 5'-CC ATC GAT ACC ATG GCG ACA GTG GCG GAG CAG-3' and 5'-CG GAA TTC CTA CAA CAG CAC AGC CTG GGC-3'. The PCR product was then subcloned into the CS2- vector through *Clal* and *EcoRI* restriction sites, and sequence integrity was confirmed by automated chain-termination methods.

**LCB2 cDNA.** The CS2-LCB2 construct was obtained and characterized by analogous procedures using the following primers: 5'-CC ATC GAT ACC ATG CGG CCG GAG CCC GGA GGC-3' and 5'-CG GAA TTC TCA GTC TTC TGT CTC TTC ATA-3'.

#### In vitro transcription/translation of LCB1 and LCB2

The LCB1 and LCB2 proteins were obtained by *in vitro* transcription and translation of the CS2-LCB1 and CS2-LCB2 plasmid constructs, using an SP6 polymerase-coupled rabbit reticulocyte lysate system (Promega) as indicated by Promega protocols. Both nonradioactive and radioactive translation products were generated using cold or [<sup>35</sup>S]-labeled methionine (Amersham) in the presence of RNasin ribonuclease inhibitor (Promega). To compare the p51 and LCB1 proteins, samples of affinity matrix-associated proteins and [<sup>35</sup>S]-labeled LCB1 were analyzed by SDS-PAGE (10% acrylamide gel). The separated proteins were visualized by silver staining and dehydrated onto Whatman filter paper for autoradiography. The p55 and LCB2 proteins were similarly resolved by SDS-PAGE (7.5% acrylamide gel) and visualized by western blotting using the α-LCB2 antibody (see below).

#### Mass spectrometry-based sequencing of p51 and p55

Silver stained p51 and p55 samples were subjected to in gel reduction, carboxyamidomethylation and tryptic digestion (Promega). Multiple peptide sequences were determined in a single run by microcapillary

reverse-phase chromatography directly coupled to a Finnigan LCQ quadrupole ion trap mass spectrometer equipped with a custom nano-electrospray source. The column was packed in-house with 5 cm of C18 support into a New Objective one-piece 75  $\mu$ m I.D. column terminating in a 8.5  $\mu$ m tip. Flow rate was 190 nL/min. The ion trap was programmed to acquire successive sets of three scan modes consisting of: full scan MS over alternating ranges of 395–800  $m/z$  or 800–1300  $m/z$ , followed by two data-dependent scans on the most abundant ion in those full scans. These data dependent scans allowed the automatic acquisition of a high resolution (zoom) scan to determine charge state and exact mass, and tandem mass spectroscopy (MS/MS) spectra for peptide sequence information. MS/MS spectra were acquired with a relative collision energy of 30%, an isolation width of 2.5 Da and with previously observed ions dynamically excluded from MS/MS analysis. Interpretation of the resulting MS/MS spectra of the peptides was facilitated by programs developed by the Harvard Microchemistry Facility and by database correlation with the algorithm Sequest [33,34].

#### Production of $\alpha$ -LCB1 and $\alpha$ -LCB2 polyclonal antibodies

**$\alpha$ -LCB1 antibody.** The peptide Ac-CGSTGSREKDVLLQAI-NH<sub>2</sub> (CG and LCB1 residues 401–415; 2.19 mg, 1  $\mu$ mole) was conjugated to maleimide-functionalized keyhole limpet hemocyanin (KLH; 2 mg, 0.7  $\mu$ mole maleimide) as described in the Imject protocols by its supplier (Pierce). Purification by size exclusion chromatography yielded 3 ml of KLH-peptide conjugate, which was flash frozen and stored at  $-20^{\circ}\text{C}$  until rabbit immunization. Bleeds were obtained at appropriate intervals, allowed to clot on ice, and then centrifuged at 3000 g for 10 min. The serum was subsequently removed, flash frozen, and stored at  $-78^{\circ}\text{C}$ .

**$\alpha$ -LCB2 antibody.** Antisera for the LCB2 protein was obtained through analogous methods using the peptide Ac-CGKYSRHRLVPLDRPF-NH<sub>2</sub> (CG and LCB2 residues 536–550).

#### Characterization of p51 and p55 by western blotting

Antisera and preimmune sera from rabbits were used for western blotting analyses as described in the ECL protocols by its supplier (Amersham). Matrix-associated proteins were separated by SDS-PAGE (7.5% acrylamide gels) and transferred to PDVF membranes (Immobilon P, Millipore). All incubations and washes were conducted with either PBS-T buffer (PBS, pH 7.4; 0.05% Tween-20) or TBS-T buffer (20 mM Tris-HCl pH 7.4, 150 mM NaCl, 0.1% Tween-20). Blocking of non-specific sites was accomplished by incubating the PDVF membrane in 10% non-fat dry milk in either buffer system. The  $\alpha$ -LCB1 sera were used in a 1:20 dilution in TBS-T containing 1% non-fat dry milk, whereas the  $\alpha$ -LCB2 sera were used in a 1:250 dilution in PBS-T. The corresponding preimmune sera controls were analyzed using identical conditions. Donkey-derived  $\alpha$ -rabbit Ig conjugated to horseradish peroxidase (Amersham) was used as a 1:10000 dilution with the appropriate buffer, and detection of the secondary antibody was accomplished according to the ECL protocols (Amersham).

## Acknowledgements

We thank Jing Huang for helpful discussions, and acknowledge Daniel Kirby and Kerry Pierce for their mass spectrometry expertise. The research was supported in part by the National Institute of General Medical Sciences. J.K.C. gratefully acknowledges predoctoral fellowships from the National Science Foundation and the Organic Chemistry Division of the American Chemical Society. S.L.S. is an Investigator at the Howard Hughes Medical Institute.

## References

- Craveri, R., Manachini, P.L. & Aragazzini, F. (1972). Thermozyomicidin, a new antifungal antibiotic from a thermophilic eumycete. *Experientia* **28**, 867–868.
- Kluepfel, D., et al., & Vezina, C. (1972). Myriocin, a new antifungal antibiotic from *Myriococcum albomyces*. *J. Antibiot.* **25**, 109–115.
- Fujita, T., et al., & Okumoto, T. (1994). Fungal metabolites. Part 11. A potent immunosuppressive activity found in *Isaria sinclairii* metabolite. *J. Antibiot.* **47**, 208–215.
- Sasaki, S., et al., & Fujita, T. (1994). Fungal metabolites. Part 14. Novel potent immunosuppressants, mycostericins, produced by *Mycelia sterilia*. *J. Antibiot.* **47**, 420–433.
- Fujita, T., et al., & Hirose, R. (1995). Determination of the absolute configurations and total synthesis of new immunosuppressants, mycostericins E and G. *Tetrahedron Lett.* **36**, 8599–8602.
- Fujita, T., et al., & Chiba, K. (1996). Determination of absolute configuration and biological activity of new immunosuppressants, mycostericins D, E, F, and G. *J. Antibiot.* **49**, 846–853.
- Nakamura, S., Kozutsumi, Y., Sun, Y., Miyake, Y., Fujita, T. & Kawasaki, T. (1996). Dual roles of sphingolipids in signaling of the escape from and onset of apoptosis in a mouse cytotoxic T-cell line, CTLL-2. *J. Biol. Chem.* **271**, 1255–1257.
- Horvath, A., Sutterlin, C., Manning-Krieg, U., Movva, N.R. & Riezman, H. (1994). Ceramide synthesis enhances transport of GPI-anchored proteins to the Golgi apparatus in yeast. *EMBO J.* **13**, 3687–3695.
- Miyake, Y., Kozutsumi, Y., Nakamura, S., Fujita, T. & Kawasaki, T. (1995). Serine palmitoyltransferase is the primary target of a sphingosine-like immunosuppressant, ISP-1/myriocin. *Biochem. Biophys. Res. Commun.* **211**, 396–403.
- Braun, P.E. & Snell, E.E. (1967). The biosynthesis of dihydrosphingosine in cell-free preparations of *Hansenula ciferri*. *Proc. Natl Acad. Sci. USA* **58**, 298–303.
- Brady, R.S. & Koval, G.J. (1958). The enzymatic synthesis of sphingosine. *J. Biol. Chem.* **233**, 26–31.
- Braun, P.E., Morell, P. & Radin, N.S. (1970). Synthesis of C18- and C20-dihydrosphingosines, ketodihydrosphingosines, and ceramides by microsomal preparations from mouse brain. *J. Biol. Chem.* **245**, 335–341.
- Lev, M. & Milford, A.F. (1981). The 3-ketodihydrosphingosine synthetase of *Bacteroides melaninogenicus*: partial purification and properties. *Arch. Biochem. Biophys.* **212**, 424–431.
- Williams, R.D., Wang, E. & Merrill, A.H., Jr. (1984). Enzymology of long-chain base synthesis by liver: characterization of serine palmitoyltransferase in rat liver microsomes. *Arch. Biochem. Biophys.* **228**, 282–291.
- Ghosh, T.K., Bian, J. & Gill, D.L. (1990). Intracellular calcium release mediated by sphingosine derivatives generated in cells. *Science* **248**, 1653–1656.
- Olivera, A. & Spiegel, S. (1993). Sphingosine-1-phosphate as second messenger in cell proliferation induced by PDGF and FCS mitogens. *Nature* **365**, 557–560.
- Van Brocklyn, J.R., et al., & Spiegel, S. (1998). Dual actions of sphingosine 1-phosphate: extracellular through the Gi-coupled receptor Edg-1 and intracellular to regulate proliferation and survival. *J. Cell Biol.* **142**, 229–240.
- Flores, I., Martinez, A.C., Hannun, Y.A. & Merida, I. (1998). Dual role of ceramide in the control of apoptosis following IL-2 withdrawal. *J. Immunol.* **160**, 3528–3533.
- Fujita, T., Hirose, R., Hamamichi, N. & Kitao, Y. (1995). 2-Substituted 2-aminoethanol: minimum essential structure for immunosuppressive activity of ISP-1 (myriocin). *Bioorg. Med. Chem. Lett.* **5**, 1857–1860.
- Fujita, T., et al., & Arita, M. (1996). Potent immunosuppressants, 2-alkyl-2-aminopropane-1,3-diols. *J. Med. Chem.* **39**, 4451–4459.
- Kobayashi, S., Furuta, T., Hayashi, T., Nishijima, M. & Hanada, K. (1998). Catalytic asymmetric syntheses of antifungal sphingofungins and their biological activity as potent inhibitors of serine palmitoyltransferase (SPT). *J. Am. Chem. Soc.* **120**, 908–919.
- van Echten, G., Birk, R., Brenner-Weiss, G., Schmidt, R.R. & Sandhoff, K. (1990). Modulation of sphingolipid biosynthesis in primary cultured neurons by long chain bases. *J. Biol. Chem.* **265**, 9333–9339.
- Kolter, T., van Echten-Deckert, G. & Sandhoff, K. (1994). Synthesis of sphinganine analogues modified in the head group. *Tetrahedron* **50**, 13425–13432.
- Wells, G.B. & Lester, R.L. (1983). The isolation and characterization of a mutant strain of *Saccharomyces cerevisiae* that requires a long-chain base for growth and for synthesis of phosphosphingolipids. *J. Biol. Chem.* **258**, 10200–10203.
- Buede, R., Rinker-Schaffer, C., Pinto, W.J., Lester, R.L. & Dickson, R.C. (1991). Cloning and characterization of LCB1, a *Saccharomyces* gene required for biosynthesis of the long-chain base component of sphingolipids. *J. Bacteriol.* **173**, 4325–4332.
- Nagiec, M.M., Baltisberger, J.A., Wells, G.B., Lester, R.L. & Dickson, R.C. (1994). The LCB2 gene of *Saccharomyces* and the related LCB1 gene encode subunits of serine palmitoyltransferase, the initial enzyme in sphingolipid synthesis. *Proc. Natl Acad. Sci. USA* **91**, 7899–7902.
- Weiss, B. & Stoffel, W. (1997). Human and murine serine-palmitoyl-CoA transferase – cloning, expression and characterization of the key enzyme in sphingolipid synthesis. *Eur. J. Biochem.* **249**, 239–247.
- Hanada, K., Hara, T., Nishijima, M., Kuge, O., Dickson, R.C. & Nagiec, M.M. (1997). A mammalian homolog of the yeast LCB1 encodes a component of serine palmitoyltransferase, the enzyme catalyzing the first step in sphingolipid synthesis. *J. Biol. Chem.* **272**, 32108–32114.



29. Lee, M.-J., *et al.*, & Hla, T. (1998). Sphingosine 1-phosphate as a ligand for the G protein-coupled receptor EDG-1. *Science* **279**, 1552-1554.
30. Fujita, T., *et al.*, & Okumoto, T. (1994). Fungal metabolites. Part 12. Potent immunosuppressant, 14- deoxomyriocin, (2S,3R,4R)-(E)-2-amino-3,4-dihydroxy-2- hydroxymethyleicos-6-enoic acid and structure-activity relationships of myriocin derivatives. *J. Antibiot.* **47**, 216-224.
31. Yoshikawa, M., Yokokawa, Y., Okuno, Y., Yagi, N. & Murakami, N. (1995). Syntheses, immunosuppressive activity, and structure-activity relationships of myriocin analogs, 2-epi-myriocin, 14-deoxomyriocin, Z-14-deoxomyriocin, and nor-deoxomyriocins. *Chem. Pharm. Bull.* **43**, 1647-1653.
32. Mandon, E.C., Ehses, I., Rother, J., van Echten, G. & Sandhoff, K. (1992). Subcellular localization and membrane topology of serine palmitoyltransferase, 3-dehydrosphinganine reductase, and sphinganine N- acyltransferase in mouse liver. *J. Biol. Chem.* **267**, 11144-11148.
33. Eng, J.K., McCormick, A.L. & Yates, J.R.I. (1994). An approach to correlate tandem mass spectral data with peptides with amino-acid sequences in a protein database. *J. Am. Soc. Mass. Spectrom.* **5**, 976-989.
34. Chittum, H.S., *et al.*, & Hatfield, D.L. (1998). Rabbit  $\beta$ -globin is extended beyond its UGA stop codon by multiple suppressions and translational reading gaps. *Biochemistry* **37**, 10866-10870.
35. Krishnangkura, K. & Sweeley, C.C. (1976). Studies on the mechanism of 3-ketosphinganine synthetase. *J. Biol. Chem.* **251**, 1597-1602.
36. Di Mari, S.J., Brady, R.N. & Snell, E.E. (1971). Biosynthesis of sphingolipid bases. IV. The biosynthetic origin of sphingosine in *Hansenula ciferrii*. *Arch. Biochem. Biophys.* **143**, 553-565.
37. Zweerink, M.M., Edison, A.M., Wells, G.B., Pinto, W. & Lester, R.L. (1992). Characterization of a novel, potent, and specific inhibitor of serine palmitoyltransferase. *J. Biol. Chem.* **267**, 25032-25038.
38. Cuvillier, O., *et al.*, & Spiegel, S. (1996). Suppression of ceramide-mediated program cell death by sphingosine 1-phosphate. *Nature* **381**, 800-803.
39. Mandala, S.M., *et al.*, & Spiegel, S. (1998). Sphingoid base 1-phosphate phosphatase: a key regulator of sphingolipid metabolism and stress response. *Proc. Natl Acad. Sci. USA* **95**, 150-155.
40. Zhang, H., Buckley, N.E., Gibson, K. & Spiegel, S. (1990). Sphingosine stimulates cellular proliferation via a protein kinase C-independent pathway. *J. Biol. Chem.* **265**, 76-81.
41. Zhang, H., Desai, N.N., Olivera, A., Seki, T., Brooker, G. & Spiegel, S. (1991). Sphingosine-1-phosphate, a novel lipid, involved in cellular proliferation. *J. Cell Biol.* **114**, 155-167.
42. Schroeder, J.J., Crane, H.M., Xia, J., Liotta, D.C. & Merrill, A.H., Jr. (1994). Disruption of sphingolipid metabolism and stimulation of DNA synthesis by fumonisin B1. A molecular mechanism for carcinogenesis associated with *Fusarium moniliforme*. *J. Biol. Chem.* **269**, 3475-3481.
43. Sabbadini, R.A., Betto, R., Teresi, A., Fachechi-Cassano, G. & Salvati, G. (1992). The effects of sphingosine on sarcoplasmic reticulum membrane calcium release. *J. Biol. Chem.* **267**, 15475-15484.
44. Pushkareva, M.Y., Khan, W.A., Alessenko, A.V., Sahyoun, N. & Hannun, Y.A. (1992). Sphingosine activation of protein kinases in Jurkat T cells. *J. Biol. Chem.* **267**, 15246-15251.
45. Hung, W.-C. & Chuang, L.-Y. (1996). Induction of apoptosis by sphingosine 1-phosphate in human hepatoma cells is associated with enhanced expression of bax gene product. *Biochem. Biophys. Res. Commun.* **229**, 11-15.
46. Sakakura, C., Sweeney, E.A., Shirahama, T., Hakomori, S. & Igarashi, Y. (1996). Suppression of Bcl-2 gene expression by sphingosine in the apoptosis of human leukemic HL-60 cells during phorbol ester-induced terminal differentiation. *FEBS Lett.* **379**, 177-180.
47. Shirahama, T., *et al.*, & Igarashi, Y. (1997). Sphingosine induces apoptosis in androgen-independent human prostatic carcinoma DU-145 cells by suppression of bcl-X<sup>L</sup> gene expression. *FEBS Lett.* **407**, 97-100.
48. Schmelz, E.M., Dombrink-Kurtzman, M.A., Roberts, P.C., Kozutsumi, Y., Kawasaki, T. & Merrill, A.H., Jr. (1998). Induction of apoptosis by fumonisin B1 in HT29 cells is mediated by the accumulation of endogenous free sphingoid bases. *Toxicol. Appl. Pharmacol.* **148**, 252-260.
49. Furuya, S., Mitoma, J., Makino, A. & Hirabayashi, Y. (1998). Ceramide and its interconvertible metabolite sphingosine function as indispensable lipid factors involved in survival and dendritic differentiation of cerebellar Purkinje cells. *J. Neurochem.* **71**, 366-377.
50. Suzuki, S., Lli, X.-K. & Shinomiya, T. (1996). A new immunosuppressant, FTY720, induces bcl-2-associated apoptotic cell death in human lymphocytes. *Immunology* **89**, 518-523.
51. Chiba, K., *et al.*, & Hoshino, Y. (1998). FTY720, a novel immunosuppressant, induces sequestration of circulating mature lymphocytes by acceleration of lymphocyte homing in rats. I. FTY720 selectively decreasing the number of circulating mature lymphocytes by acceleration of lymphocyte homing. *J. Immunol.* **160**, 5037-5044.
52. Yanagawa, Y., Sugahara, K., Kataoka, H., Kawaguchi, T., Masubuchi, Y. & Chiba, K. (1998). FTY720, a novel immunosuppressant, induces sequestration of circulating mature lymphocytes by acceleration of lymphocyte homing in rats. II. FTY720 prolongs skin allograft survival by decreasing T cell infiltration into grafts but not cytokine production. *J. Immunol.* **160**, 5493-5499.
53. Stoffel, W. & Bister, K. (1973). Stereospecificities in the metabolic reactions of the four isomeric sphinganine (dihydrosphingosine) in rat liver. *Hoppe Seylers Z. Physiol. Chem.* **354**, 169-181.
54. Shimeno, H., Soeda, S., Sakamoto, M., Kouchi, T., Kowakame, T. & Kihara, T. (1998). Partial purification and characterization of sphingosine N-acyltransferase (ceramide synthase) from bovine liver mitochondrion-rich fraction. *Lipids* **33**, 601-605.
55. Stoffel, W., Sticht, G. & LeKim, D. (1969). Metabolism of sphingosine bases. X. Degradation of [1-<sup>14</sup>C]dihydrosphingosine (sphinganine), [1-<sup>14</sup>C]2-amino-1,3-dihydroxyheptane and [1-<sup>14</sup>C]dihydrosphingosine phosphate in rat liver. *Hoppe Seylers Z. Physiol. Chem.* **350**, 63-68.
56. Stoffel, W., Assmann, G. & Binczek, E. (1970). Metabolism of sphingosine bases. XIII. Enzymatic synthesis of 1-phosphate esters of 4t-sphingenine (sphingosine), sphinganine (dihydrosphingosine), 4-hydroxysphinganine (phytosphingosine) and 3- dehydrosphinganine by erythrocytes. *Hoppe Seylers Z. Physiol. Chem.* **351**, 635-642.
57. van Echten-Deckert, G., *et al.*, & Sandhoff, K. (1997). cis-4-Methylsphingosine decreases sphingolipid biosynthesis by specifically interfering with serine palmitoyltransferase activity in primary cultured neurons. *J. Biol. Chem.* **272**, 15825-15833.
58. Humpf, H.-U., *et al.*, & Merrill, A.H., Jr. (1998). Acylation of naturally occurring and synthetic 1-deoxysphinganine by ceramide synthase. *J. Biol. Chem.* **273**, 19060-19064.

---

**Because Chemistry & Biology operates a 'Continuous Publication System' for Research Papers, this paper has been published via the internet before being printed. The paper can be accessed from <http://biomednet.com/cbiology/cmb> – for further information, see the explanation on the contents pages.**